

First-principles determination of the bulk phase diagram for body-centered-tetragonal copper: Application to epitaxial growth of Cu on Fe{100}

I. A. Morrison

Department of Materials Science and Engineering and The Laboratory for Research on the Structure of Matter, University of Pennsylvania, Philadelphia, Pennsylvania 19104

M. H. Kang and E. J. Mele

Department of Physics and The Laboratory for Research on the Structure of Matter, University of Pennsylvania, Philadelphia, Pennsylvania 19104

(Received 30 June 1988)

From the results of our *ab initio* pseudopotential total-energy calculation on Cu in the body-centered-tetragonal (bct) crystal system, a first-principles phase diagram for bulk bct Cu is derived as a function of externally applied stresses. An interesting fcc-to-bcc structural transition is predicted, induced by the application of a biaxial tension and a hydrostatic pressure. The biaxial tension needed to initiate the transformation is found, however, to be too large to attain macroscopically without inducing plastic flow (i.e., dislocation motion) in single crystal copper. An explanation for the existence of a metastable (albeit rather disordered) phase of bcc Cu on an iron substrate, recently observed by Wang *et al.*, is put forth by considering the energy of tetragonal distortions on the cubic phases of Cu. The results of our *bulk* bct calculations suggest that the disorder observed on Cu/Fe{100} is due to a nonoptimal match of lattice constants. The growth of a stable bct phase of Cu on a suitable cubic substrate with lattice constant 2.76 Å may be possible.

Molecular-beam epitaxy (MBE) and other modern surface-science techniques allow the synthesis of metastable phases of materials with structural and/or magnetic properties not found in the bulk. The transition metals are of particular interest, showing a regular hcp-bcc-hcp-fcc bulk structural trend as the *d* band is filled, in addition to a wide range of metastable structural and magnetic properties upon epitaxial growth. The advent of tractable *ab initio* electronic structure methods, employing the local-density approximation (LDA) for the exchange-correlation energy of an interacting homogeneous electron gas, allow one to accurately study such systems and are a powerful tool in the interpretation of experimental data. The transition metals have been studied extensively using various LDA calculations, e.g., the all-electron full-potential linear augmented-plane-wave (FLAPW) method,¹ the Korringa-Kohn-Rostoker (KKR) method,² the augmented-spherical-wave (ASW) method,³ the linearized muffin-tin orbital (LMTO) method,⁴ and the pseudopotential method. Unlike other *ab initio* methods, however, the pseudopotential method has traditionally been rather difficult to apply to the 3*d* transition metals with great accuracy because of the highly localized nature of the 3*d* charge distribution.

We have recently introduced a real space formulation of the mixed-basis (MB) pseudopotential method⁵ that extends the *ab initio* pseudopotential method to study of the 3*d* transition metals. This modified MB method was applied to the study of elemental copper in the fcc and bcc structures. At all densities studied, the fcc phase was found to be energetically favored and no hydrostatic pressure-induced phase transition between fcc and bcc was predicted. For fcc copper, the lattice constant, bulk

modulus, and cohesive energy were calculated to within 0.6%, 6%, and 4.5% of the experimental values, respectively. The calculated band structure compared well with photoemission data and, overall, the results were in good agreement and of comparable accuracy to other all-electron *ab initio* results.

Recent experimental data has caused us to reconsider the fcc-bcc copper problem. Wang *et al.*⁶ reported a low-energy electron diffraction (LEED) analysis of epitaxially grown copper (~12–25 monolayers) on a Fe{001} substrate that suggests the film, although rather disordered, contains a detectable phase of “somewhat distorted” bcc copper. In support of their conclusion, they cite the ASW spin-polarized band calculation of Marcus *et al.*⁷ that predicts a zero-temperature lattice constant of 2.87 Å for bcc Cu and 2.82 Å for bcc Fe. Based on these results, the bcc modifications of Cu and Fe would appear to be ideal epitaxy partners, with the Cu lattice compressed by only 1.8%.

A continuum elasticity model based on Landau theory has been developed by Bruinsma and Zangwill⁸ to explain the behavior of such strained epitaxial metal overlayers. Here we consider the problem from a more microscopic point of view and put forth an explanation for the existence of this metastable phase of Cu by considering the energy of tetragonal distortions on the *bulk* fcc and bcc phases of Cu. The previous calculation, which considered the stability of the fcc and bcc phases of Cu under the application of a purely hydrostatic pressure, was not sufficiently general to make any comment on the behavior of Cu under the application of a nonuniform stress. Therefore, to examine this question in more detail, we extend the previous work to examine the stability of a con-

tinuous range of structures between fcc and bcc within the body-centered-tetragonal (bct) crystal system, where fcc and bcc are special high-symmetry structures of the lower-symmetry bct lattice. Figure 1 shows the relationship between a general face-centered-tetragonal (fct) and bct unit cell. The lattices are equivalent to each other and differ only by a rotation of 45° about the c axis. Note that for $c/a=1$, the bct lattice reduces to a bcc lattice and for $c/a=\sqrt{2}$, the rotated bct lattice reduces to a fcc lattice. Thus a variation of the c/a ratio allows one to go continuously from the bcc to fcc structure, all within the same crystal system.

The rationale for examining copper in the hypothetical bct crystal system is the possibility it affords for considering more general stress-induced phase transformations. Most *ab initio* calculations consider energy as a function of uniform compression and expansion. This volume variation simulates the application of the conjugate thermodynamic field, $-\partial E/\partial V$, or pressure. Energy versus volume curves thus allow one to examine the relative stability of various phases of a material under the application of hydrostatic pressure. The addition of an extra degree of structural freedom in the bct system (independent variations of c and a) allows one to introduce a second conjugate thermodynamic field, in addition to the hydrostatic pressure. Coupled with a knowledge of the total energy variations of such a system, these fields can serve as useful tools to probe possible structural phase transitions induced by anisotropic stresses.

The present calculation employs the usual plane-wave basis set augmented with a localized basis of "optimized" d functions⁵ that are constructed to be rigorously *nonoverlapping* in the solid state. Thus, unlike the conventional MB method,⁹ matrix elements and parts of the charge density involving the localized functions are evaluated directly in real space by very fast and accurate one-dimensional integrals. We employ an *ab initio* non-local pseudopotential derived by Bachelet *et al.*¹⁰ to represent the copper valence electron-ion interaction and use the results of Ceperley and Alder¹¹ for the local-density ap-

proximation in the parametrized form given by Perdew and Zunger.¹² The total energy is calculated in the momentum-space formalism of Ihm, Zunger, and Cohen.¹³ Recently, this formalism was successfully applied to the study of the structural properties of bulk NiAl and the NiAl(110) surface.¹⁴

Since a satisfactory convergence test with respect to the various energy cutoff parameters was performed in the previous study of cubic copper,⁵ those values were reused in the present calculation (except the \mathbf{k} -point sampling) and were found to yield the same total energy, Fermi level, eigenvalues, etc., for the bcc and fcc structures *within the bct system*. To simplify the thinking about the shape of the real and reciprocal primitive cells as c and a are varied, we chose to model the bct crystal as a simple tetragonal (st) lattice with a two-point basis (the point group for both the st and bct lattices is D_{4h} , with 16 point operations). We use a plane-wave basis set of about 160 plane waves ($|\mathbf{k}+\mathbf{G}|_{\max}^2=15$ Ry), a localized basis set of ten optimized d functions (five functions per Cu atom); 6000 plane waves to expand the relatively smooth local potential ($|\mathbf{G}_{\max}|^2=169$ Ry), and 24 000 plane waves to expand the charge density ($|\mathbf{G}|_{\max}^2=430$ Ry). The charge density is accumulated on 27 \mathbf{k} points in the irreducible Brillouin zone (128 \mathbf{k} points in the full BZ) and the Fermi level is calculated by the usual Gaussian weighting technique,¹⁵ which stabilizes the total energy with respect to the number of \mathbf{k} points. The total energies and self-consistent potentials are converged to within 0.01 and 0.5 mRy, respectively.

The cutoff radius, r_c , for the nonoverlapping d functions is chosen as 2.25 a.u. (as in Ref. 5). This fixed radius naturally restricts the degree to which a given structure can be compressed and at all times the nearest-neighbor distance is required to be greater than $2r_c$. For the bct lattice, there are three distinct regions of nearest-neighbor distance, d_{NN} : (1) $c/a \leq \sqrt{2}/3$, $d_{\text{NN}}=c$; (2) $\sqrt{2}/3 < c/a < \sqrt{2}$, $d_{\text{NN}}=0.5(c^2+2a^2)^{1/2}$; (3) $c/a \geq \sqrt{2}$, $d_{\text{NN}}=a$.

Figure 2 shows a contour plot of our calculated total

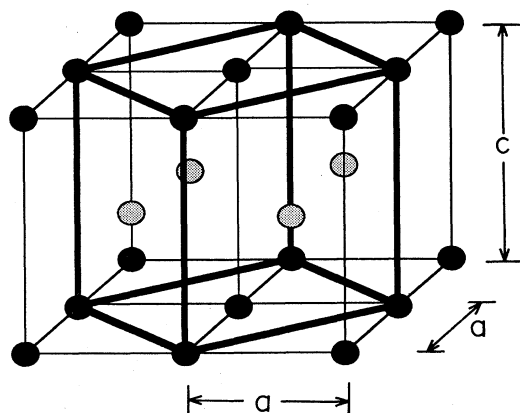


FIG. 1. Relationship between the bct and rotated fct unit cells. Shown are four bct unit cells, whose body-centered atoms are lightly shaded for clarity. These atoms also function as face-centered atoms for the rotated fct unit cell.

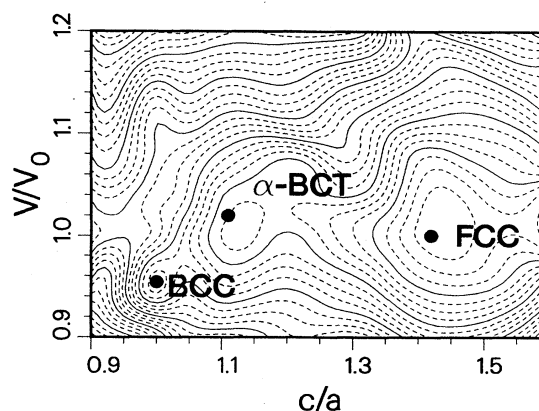


FIG. 2. Contour plot of total energy surface for bct Cu as a function of c/a vs V/V_0 . Contour spacing is 0.5 mRy. The fcc, α -bct, and bcc equilibrium structures, as shown in Fig. 4, are marked.

energy surface for Cu in the bct system, with constant-energy contours separated by 0.5 mRy. The independent structural parameters are chosen as c/a and V/V_0 , where V is the unit-cell volume ($V=0.5ca^2$) and V_0 is the experimental fcc Cu unit-cell volume ($V_0=79.37$ a.u.³). The energy surface is a quintic interpolation generated from the results of 70 self-consistent structure calculations. The numerically interpolated contour plot has three distinguishing features: a global minimum on the fcc structure line (at $c/a=1.43$, $V/V_0=1.02$) and two local minima, one on the bcc line (at $c/a=1.0$, $V/V_0=0.95$) and the other on an intermediate structure, labeled " α -bct" for reference (at $c/a=1.12$, $V/V_0=1.0$). Note that the fcc global minimum represents a 1.1% error in c/a and 1.1% error in volume ratio when compared to the experimental fcc copper structure. The relative energies per atom for the two local minima are found to be $E(\alpha\text{-bct})-E(\text{fcc})=+3.2$ mRy, and $E(\text{bcc})-E(\text{fcc})=+4.8$ mRy.

Besides the three principal minima, the surface also exhibits considerable fine structure, which most likely is not physical but rather may result from some limitation in the choice of localized basis functions used to represent the highly localized d electrons. Nevertheless, we believe the overall shape of the surface and the placement of the minima are correct. As will be discussed below, the final results were found to be rather insensitive to the fine structure.

The total energy curves for Cu in the fcc and bcc structures, as calculated within the bct system (Fig. 3), are identical to the previous results for Cu as calculated with the *cubic* system.⁵ The curious bimodal shape of the bcc curve, reported previously,⁵ is reproduced in this lower-symmetry crystal environment and has been previously

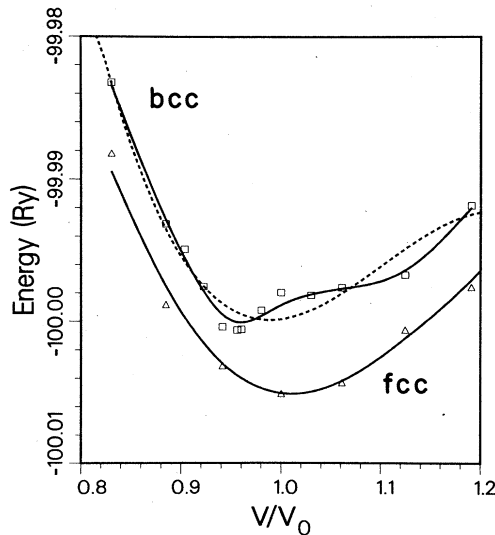


FIG. 3. The total energy curves (per atom) for fcc and bcc Cu in the bct crystal system. The triangles (squares) represent the calculated fcc (bcc) data points. The solid curves are obtained by a spline smoothing algorithm. The dashed curve is a least-squares fit of a fourth-order polynomial to the bcc data points.

associated with a symmetry breaking of the filled Cu d band under compression.⁵ The energy surface results show, however, that the shallow "minimum" is not really a minimum, but rather is part of a local plateau region in the energy surface. A fourth-order polynomial least-squares fit to the bcc data points (Fig. 3, dashed curve) yields a minimum V/V_0 of 0.98 and a bulk modulus of 1.26 Mbar. For comparison, Chelikowsky and Chou¹⁶ find a bcc Cu bulk modulus of 1.85 Mbar and a V/V_0 minimum of 1.0 using the Gaussian orbitals [linear combination of atomic orbitals (LCAO)] pseudopotential method.¹⁷

In addition to the work of Bruinsma and Zangwill,⁸ the bct structural transformation has been studied previously by several authors,¹⁸ although usually within the framework of linear elasticity theory and/or a pair-potential formalism. Such methods, while very useful, lack the accuracy needed to distinguish the subtle energy differences that result as c and a varied. The *ab initio* nature of our calculation allows us to map the total energy surface of the system very accurately and to consider the possibility of a zero-temperature phase transition between fcc and bcc Cu induced by external stresses. For later convenience in constructing such a phase diagram, we define the extensive thermodynamic variables as V and a^2 , and then introduce the natural conjugate thermodynamic fields, P , the applied hydrostatic pressure, and μ , the external biaxial surface tension. We then may construct the zero-temperature Gibbs free energy per atom of the system, for a given external P and μ , as follows:

$$G = E + PV + \mu a^2,$$

where E is the total electronic energy per atom in the pseudopotential framework and the last two terms represent the external mechanical energy. Dimensionally, μ is a surface tension, or force per unit length, with a negative value of μ corresponding to a uniform expansion along the a axis of the crystal. For a given P and μ , the minimum value of G , for all V and a^2 values considered, represents the equilibrium state of the system. Thus by systematically varying the external fields and tracking the equilibrium structure, we map out the phase diagram for the system (Fig. 4).

It is important to note that the nature of the phase diagram is dominated by the three principal minima in the surface and is quite insensitive to the fine structure or "wiggles" discussed above. Also, the shape of the phase diagram was also found to be rather insensitive to the exact details of the surface fitting algorithm.

Note that for $\mu=0$, we confirm the previous result that fcc Cu is stable under the application of a purely hydrostatic pressure. With no external fields ($P=\mu=0$), we have $G=E$ and the crystal prefers to sit in the fcc global minimum; however, the application of a positive P (compression) and a negative μ (expansion) can work together to lower the Gibbs free energy of the system and bring about a structural transition. For zero external hydrostatic pressure, we find at $\mu=-623$ dyn/cm, or equivalently, at $\mu/c_0=-17$ kbar (where c_0 is the equilibrium fcc Cu lattice constant of 3.61 Å), a structural transition from fcc Cu to the α -bct structure is possible. For

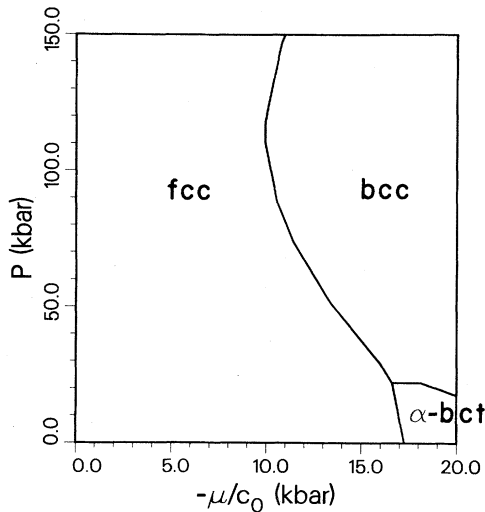


FIG. 4. Equilibrium structural phase diagram of bulk bct Cu as a function of biaxial tension vs external hydrostatic pressure. The surface tension μ has been scaled by c_0 , the equilibrium lattice constant of fcc copper ($c_0 = 3.61 \text{ \AA}$) to yield the more familiar units of kbars ($1 \text{ kbar} = 10^9 \text{ dyn/cm}^2$).

a range of hydrostatic pressures from about 20 to 170 kbar, we find a direct fcc to bcc phase transition is possible under the application of a nonzero biaxial tension, with μ/c_0 equal to at least -10 kbar. At the fcc minimum, $c = 3.62 \text{ \AA}$ and $a = 2.65 \text{ \AA}$, and at the bcc minimum, $c = 2.82 \text{ \AA}$ and $a = 2.82 \text{ \AA}$. Thus, P and μ are a natural set of external thermodynamic fields in that they provide the correct mechanical forces necessary to initiate the fcc-to-bcc transition: a uniform compression of the system (provided by P) coupled with a competing biaxial pulling out along the a axes (provided by μ).

Note that the range of both the transition pressures and biaxial tensions involved in the phase diagram is relatively modest in size. One therefore might imagine that such an experiment could be performed, since pressures in the Mbar range are now readily accessible with diamond-anvil techniques. Unfortunately, the application of a biaxial tension is rather difficult to realize without inducing plastic deformation in copper. At the zero-pressure transition point, μ/c_0 is -17 kbar, whereas the minimum stress needed to plastically deform a very pure copper single crystal is only -3.4 bars (ref. 19) and may be even smaller depending on sample preparation. Thus plastic deformation (i.e., dislocation motion) occurs at stress levels 3 orders of magnitude smaller than our predicted transition pressure and hence effectively hinders the structural transition in bulk copper.

We now turn to the more interesting question of what transformations are possible in the Cu/Fe{100} epitaxy system. In this case, where the film is only a few monolayers thick, the microscopic stresses present at the interface can be many times larger than the yield stress of the material, so the above argument on the plastic flow of Cu will not be relevant. Although a rigorous treatment of the Cu/Fe{100} system really requires a separate

ab initio supercell calculation, the results of the present study (carried out for bulk bct Cu) are fairly easily reinterpreted in light of the epitaxy problem and provide a sufficiently reasonable explanation for the observed results of Wang *et al.* to merit consideration. With this caveat in mind, we proceed as follows.

The first question to consider is whether the experimental results of Wang *et al.* are understandable in terms of the derived phase diagram (Fig. 4). Although the experiment is carried out at zero external hydrostatic pressure, there is no way to estimate the biaxial stress present at the surface and therefore no way to isolate the location of the structure on the phase diagram. It is not even clear if such an association between a metastable epitaxial overlayer and a bulk equilibrium phase diagram is meaningful. Also, it is important to realize that the phase diagram represents the situation where c and a are allowed to vary independently so as to minimize the free energy for a given externally applied P and μ . While this may be an appropriate set of constraints for a bulk sample, a more natural constraint for the epitaxy situation is to fix the in-plane lattice constant a to match the underlying substrate. Since the bulk modulus for Fe at 4.2 K is 1.73 Mbar compared to 1.42 Mbar for Cu at 0 K,²⁰ it is reasonable to expect the Fe substrate to be stiffer than the Cu overlayer.

The relevant information to consider, therefore, is the energy variation of Cu as a function of c , the lattice parameter perpendicular to the interface, for a fixed in-plane lattice constant a . This information is already contained within the calculated energy surface and is readily extracted. Consider three slices of the energy as a function of c , or equivalently, V/V_0 , for a fixed in-plane lattice constant a , with $a = 2.86, 2.76$, and 2.56 \AA [Fig. 5(a)]. These values correspond to a_{Fe} , the 0 K lattice constant for Fe,²¹ and the a values at the α -bct and fcc minima, respectively. Figure 5(b) shows the structure path that these slices represent with respect to the energy surface. Note that the α -bct structure shown in the phase diagram (Figs. 2 and 4) does not lie on the exact minimum of the shallow total energy well near the $c/a = 1.1$ line, but rather lies slightly off to one side. This is reasonable, since in the construction of the phase diagram one seeks the minimum of the Gibbs free energy, which need not necessarily correspond to the minimum of the internal energy. Nevertheless, for simplicity of notation, we shall refer to both the exact numerical minimum at $c/a = 1.12$ and $V/V_0 = 1.0$ [$a = 2.76 \text{ \AA}$, point C in Figs. 5(a) and 5(b)] and the equilibrium bulk phase at $c/a \cong 1.11$ and $V/V_0 \cong 1.02$ ($a = 2.79 \text{ \AA}$, Figs. 2 and 4) as the α -bct structure since they are both associated with shallow minimum near $c/a = 1.1$.

Now consider the layer-by-layer growth mechanism for the Cu/Fe{100} system. The reference point for this discussion will be the 5 structures labeled A-E in Figs. 5(a) and 5(b). The first layer grows as a square lattice with $a = a_{\text{Fe}}$ with little or no strain because of the near-perfect lattice match between substrate and overlayer. Since the c lattice constant is not constrained as the second layer grows, the system forms its minimum-energy structure, subject to the boundary condition at the interface (point

B). Note that the bcc phase (point *A*) is not the equilibrium (i.e., minimum-energy) structure, nor is it found to be for any *a* value, although for $a=2.83$ Å the two minima *A* and *B* are of equal depth. For increasing or decreasing *a* values, however, the minimum associated with point *B* is lower in energy. As with the bulk bct phase diagram, the bcc phase can be stabilized by the application of an external uniaxial pressure, this time perpendicular to the interface. A common tangent construction between the points *A* and *B* yields a uniaxial pressure of approximately 23 kbar necessary to stabilize the bcc phase. With respect to small negative distortions in the in-plane lattice constant *a*, the *B* structure is clearly not a stable minimum and as a result, as the layer grows, the lattice would prefer to transform to the nearby stable local structure, the α -bct structure (point *C*). This structure, however, has an in-plane lattice constant *a* different by 4% from the lower Cu layers and substrate. The epitaxial layer thus grows more strained as additional monolayers are deposited and eventually the strain mismatch becomes too large for the substrate to support. The Cu overlayer then distorts and grows in an incommensurate

and disordered fashion. The calculation suggests that the ordered component of the Cu overlayer is predominantly a strained body-centered tetragonal structure with a *c/a* ratio of approximately 1.07 (point *B*) and most likely not a true bcc phase. The disorder results because the Cu and Fe lattice constants are not optimally matched for the growth of the bcc phase.

As to the possibility of growing any metastable phase of Cu epitaxially, our results suggest two possibilities: (1) for a substrate lattice constant of 2.82 Å (this intersects the bcc minimum at $V/V_0=0.95$), the application of an external uniaxial pressure on the surface could possibly stabilize the bcc phase, since the bcc minimum is a stable minimum with respect to small variations in *a*; (2) a cubic substrate with a lattice constant of 2.76 Å (to match the stable α -bct minimum) may support the growth of bct Cu with no applied uniaxial pressure.

In summary, an explanation for the existence of a metastable and disordered phase of bcc Cu on an iron substrate observed by Wang *et al.* has been put forth by considering the energy of tetragonal distortions on the fcc and bcc phases of Cu. We believe the analysis of the calculated bct energy surface in terms of a constrained in-plane lattice constant captures the essential physics of the problem and provides a reasonable explanation for the observations. Naturally, these conclusions are open to some question due to the one-component bulk nature of the calculation, but nevertheless, the energetics of bulk bct Cu do naturally suggest the suitability of such epitaxially possibilities.

The bimodal bcc Cu total energy curve (Fig. 3) differs from that obtained by Marcus *et al.*⁷ and more recently by Chelikowsky and Chou.¹⁶ Our previous work has suggested that the nearcore nonspherical charge distortion of the full Cu *d* shell is largely responsible for the anomalous bcc deep energy minimum. Whether this nonspherical distortion is physical or computational in origin, however, is not yet clear. A possible computational explanation is that under compression the bcc core region may be trying to move in such a manner that is too large to be represented by our plane wave basis set. We are currently investigating the possible inadequacy or "stiffness" of our localized basis set by extending this study to Ag. Given the quality of our fcc Cu results, however, such a core relaxation does not appear to be a problem in the face-centered cubic structure. Further independent calculations on the copper system would greatly help to clarify this situation.

We thank J. R. Chelikowsky and M. Y. Chou for sharing their results with us before publication. We also acknowledge several very useful discussions with V. Vitek on mechanical properties of metals and elasticity theory. We especially thank D. M. Wood for pointing out to us the importance of constraining the in-plane lattice constant. One of us (I.A.M.) acknowledges the support of the National Science Foundation (NSF) through the Materials Research Laboratory (MRL) program under Grant No. DMR85-19059. Two of us (M.H.K. and E.J.M.) acknowledge the support of the Department of Energy under Contract No. DE-FG02-84ER45118.

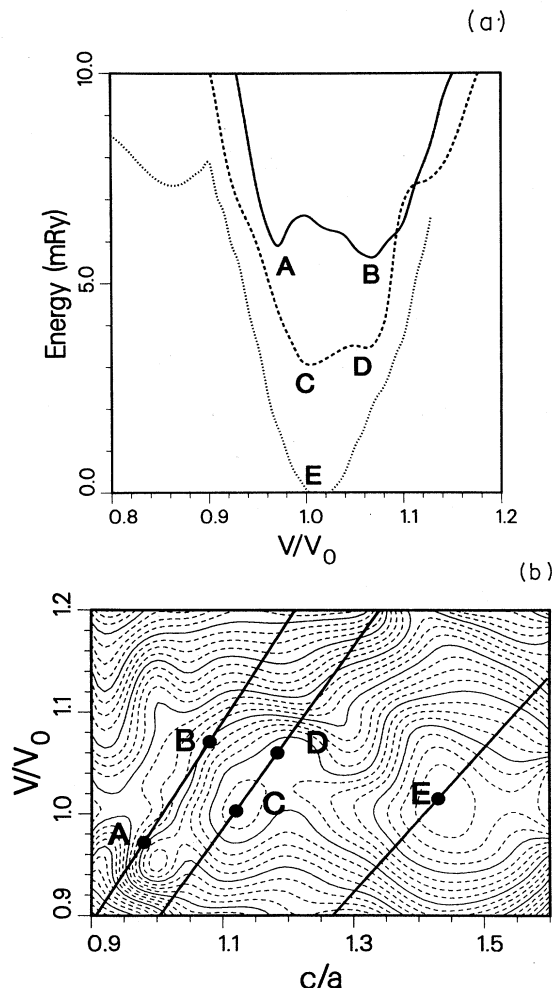


FIG. 5. (a) Energy vs volume ratio curves for fixed in-plane lattice constant *a*, with $a=2.86$ Å (solid curve), $a=2.76$ Å (dashed curve), $a=2.56$ Å (dotted curve). (b) Constant *a* lines corresponding to the energy surface cuts shown in (a).

- ¹E. Wimmer, H. Krakauer, M. Weinert, and A. J. Freeman, *Phys. Rev. B* **24**, 864 (1981).
- ²V. L. Moruzzi, J. F. Janak, and A. R. Williams, *Calculated Electronic Properties of Metals* (Pergamon, New York, 1979).
- ³A. R. Williams, J. Kübler, and C. D. Gelatt, Jr., *Phys. Rev. B* **19**, 6094 (1979).
- ⁴O. K. Andersen, *Phys. Rev. B* **12**, 3060 (1975).
- ⁵M. H. Kang, R. C. Tatar, E. J. Mele, and P. Soven, *Phys. Rev. B* **35**, 5457 (1987).
- ⁶Z. Q. Wang, S. H. Lu, Y. S. Li, F. Jona, and P. M. Marcus, *Phys. Rev. B* **35**, 9322 (1987).
- ⁷P. M. Marcus, V. L. Moruzzi, Z. Q. Wang, Y. S. Li, and F. Jona, in *Physical and Chemical Properties of Thin Metal Overlayers and Alloy Surfaces*, Vol. 83 in *Materials Research Society Symposia Proceedings*, edited by D. M. Zehner and P. W. Goodman (Materials Research Society, Pittsburgh, PA, 1987).
- ⁸R. Bruinsma and A. Zangwill, *J. Phys. (Paris)* **47**, 2055 (1983).
- ⁹S. G. Louie, K. M. Ho, and M. L. Cohen, *Phys. Rev. B* **19**, 1774 (1979).
- ¹⁰G. B. Bachelet, D. R. Hamann, and M. Schlüter, *Phys. Rev. B* **26**, 4199 (1982); **29**, 2309(E) (1984).
- ¹¹D. M. Ceperley and B. J. Adler, *Phys. Rev. Lett.* **45**, 566 (1980).
- ¹²J. P. Perdew and A. Zunger, *Phys. Rev. B* **23**, 5048 (1981).
- ¹³J. Ihm, A. Zunger, and M. L. Cohen, *J. Phys. C* **12**, 4401 (1979).
- ¹⁴M. H. Kang and E. J. Mele, *Phys. Rev. B* **36**, 7371 (1987).
- ¹⁵C. L. Fu and K. M. Ho, *Phys. Rev. B* **28**, 5480 (1983).
- ¹⁶J. R. Chelikowsky and M. Y. Chou, *Phys. Rev. B* **38**, 7966 (1988).
- ¹⁷J. R. Chelikowsky and S. G. Louie, *Phys. Rev. B* **29**, 3470 (1984).
- ¹⁸P. Beauchamp and J. P. Villain, *J. Phys. (Paris)* **44**, 1117 (1983), and references therein.
- ¹⁹R. W. K. Honeycombe, *The Plastic Deformation of Metals* (Arnold, London, 1984), p. 12.
- ²⁰G. Simmons and H. Wang, *Single Crystal Elastic Constants and Calculated Aggregate Properties: A Handbook* (MIT, Cambridge, Massachusetts, 1971).
- ²¹The 0-K lattice constant is estimated using the Fe linear expansion coefficient and the $T=20^\circ\text{C}$ lattice-constant value of 2.866 Å.